Role of hepatic glucose signaling in the development of liver disease

Lei, Yu

DOI:
10.33612/diss.126530476

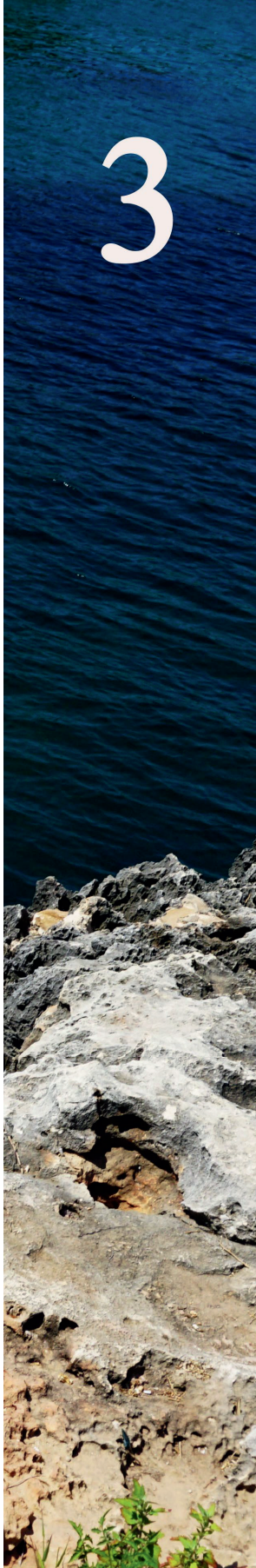

Chapter 3

Glucose-6-phosphate regulates hepatic bile acid synthesis in mice

Joanne A. Hoogerland[1], Yu Lei[1], Justina C. Wolters[1], Jan Freark de Boer[1,2], Trijnie Bos[1], Aycha Bleeker[1], Niels L. Mulder[1], Theo H. van Dijk[2], Jan A. Kuivenhoven[1], Fabienne Rajas[3], Gilles Mithieux[3], Rebecca A. Haeusler[4], Henkjan J. Verkade[1], Vincent W. Bloks[1], Folkert Kuipers[1,2] and Maaike H. Oosterveer[1]

[1]Departments of Pediatrics and [2]Laboratory Medicine, University of Groningen, University Medical Center Groningen, 9713 GZ Groningen, The Netherlands. [3]Institut National de la Santé et de la Recherche Médicale, U1213, Université Claude Bernard Lyon, 69100 Villeurbanne, France. [4]Department of Pathology and Cell Biology, Columbia University College of Physicians and Surgeons, New York, New York 10032, USA

Hepatology (2019): 70(6):2171-2184

Abstract

It is well-established that, besides facilitating lipid absorption, bile acids act as signaling molecules that modulate glucose and lipid metabolism. Bile acid metabolism, in turn, is controlled by several nutrient-sensitive transcription factors. Altered intrahepatic glucose signaling in type 2 diabetes associates with perturbed bile acid synthesis. However, an independent role of glucose in regulation of bile acid metabolism has as yet not been established. We aimed to characterize the regulatory role of the primary intracellular metabolite of glucose, glucose-6-phosphate (G6P), on bile acid metabolism. Hepatic gene expression patterns and bile acid composition were analyzed in mice that accumulate G6P in the liver, i.e., liver-specific glucose-6-phosphatase knockout (L-*G6pc*$^{-/-}$) mice, mice treated with a pharmacological inhibitor of the G6P-transporter, and in cultured cells. Hepatic G6P accumulation induces *Cyp8b1* expression, which is mediated by the major glucose-sensitive transcription factor Carbohydrate Response Element Binding Protein (ChREBP). Activation of the G6P-ChREBP-CYP8B1 axis increases the relative abundance of cholic acid-derived bile acids and induces physiologically relevant shifts in bile composition. The G6P-ChREBP-dependent change in bile acid hydrophobicity associates with elevated plasma campesterol/cholesterol ratio and reduced fecal neutral sterol loss, compatible with enhanced intestinal cholesterol absorption. ***Conclusion:*** We report that G6P, the primary intracellular metabolite of glucose, controls hepatic bile acid synthesis. Our work identifies hepatic G6P-ChREBP-CYP8B1 signaling as a regulatory axis in control of bile acid and cholesterol metabolism.

Introduction

Bile acids facilitate absorption of dietary lipids and fat-soluble vitamins in the intestine but also act as signaling molecules that control glucose, lipid and energy metabolism (1). Bile acid metabolism is known to be perturbed in conditions of uncontrolled hyperglycemia and insulin resistance (2,3). Bile acid synthesis from cholesterol occurs exclusively in the liver and comprises multiple biochemical reactions initiated by cholesterol 7α-hydroxylase (CYP7A1), the rate-controlling enzyme in the 'classic' pathway of primary bile acid synthesis. Sterol 12α-hydroxylase (CYP8B1) subsequently generates 3α,7α,12α-trihydroxy-5β-cholan-24-oic acid (cholic acid; CA) as endproduct (2,4,5). As a consequence, hepatic CYP8B1 activity determines the contribution of CA produced in the 'classic' pathway relative to 3α,7α-dihydroxy-5β-cholan-24-oic acid (chenodeoxycholic acid; CDCA). CDCA, in contrast to CA, can also be generated via an 'alternative' pathway starting with 27-hydroxylation of cholesterol (6). CDCA is efficiently converted to hydrophilic C6-hydroxylated muricholic acids (MCAs) in rodents but not in humans (6). Primary bile acid species are secreted into the intestine where they can be converted by microbial actions to secondary bile acids with distinct physicochemical properties (6) that determine their efficacy to promote fat and cholesterol absorption as well as their signaling functions (1).

Bile acid synthesis is increased during postprandial periods and reduced upon fasting (7). Insulin and glucose have both been reported to induce the expression of *CYP7A1* in cultured hepatocytes (8,9). Moreover, insulin suppresses while glucose induces the expression *Cyp8b1* (9,10). Insulin-induced suppression of *Cyp8b1* is mediated by the transcription factor Forkhead box protein O1 (FOXO1) (4). Under insulin-resistant conditions, constitutive FOXO1 activation shifts the composition of the bile acid pool towards an increased contribution of CA and its hydrophobic microbial metabolite 3α,12α-dihydroxy-5β–cholan-24-oic acid (deoxycholic acid; DCA) (4). Accordingly, we and others have shown that insulin resistance is associated with an increase in CA synthesis (2,4,5) and a more hydrophobic bile acid pool in humans (2). Insulin resistance is generally associated with hyperglycemic episodes, enhancing intrahepatic glucose metabolism (11,12). However, the contribution of increased intrahepatic glucose availability to hepatic *Cyp8b1* induction and the physiological consequences thereof have remained elusive.

Here we characterized the direct regulatory role of intrahepatic glucose on bile acid synthesis. After being taken up by hepatocytes, glucose is immediately converted into glucose-6-phosphate (G6P), the primary intracellular metabolite of glucose that acts as a signaling molecule (12). Glycogen Storage Disease type 1 (GSD I) is an inborn error of carbohydrate metabolism caused by mutations in the glucose-6-phosphatase (*G6PC*) gene (GSD Ia) or the glucose-6-phosphate transporter *SLC37A4* (GSD Ib). GSD I is characterized by a strong accumulation of G6P inside hepatocytes and, importantly, low fasting glucose and insulin levels (13). We took advantage of this unique feature to evaluate the effects of intracellular glucose *versus* blood glucose and insulin and, hence, to selectively establish the effects of intra- *versus* extrahepatic glucose on bile acid metabolism. Our data show that, in

mice, intrahepatic G6P regulates bile acid metabolism via a Carbohydrate Response Element Binding Protein (ChREBP, also known as Mlxipl)-dependent induction of CYP8B1, resulting in an increased hydrophobicity of the biliary bile acids and reduced fecal cholesterol loss. On the other hand, hepatic CYP7A1 expression was regulated by extrahepatic (blood) glucose rather than intrahepatic G6P.

Materials and Methods

Animals

Male adult (8-12 weeks) B6.*G6pc*$^{lox/lox}$ and B6.*G6pc*$^{lox/lox}$.SA$^{creERT2/w}$ mice (14) and male L-*FoxO1,3,4* mice (18-20 weeks old) (15) and C57BL/6 mice (12-13 weeks old) (own breeding) were housed in a light- and temperature-controlled facility and fed a standard laboratory chow diet (RMH-B, AB-diets, Woerden). Liver-specific *G6pc*-deficient mice (L-*G6pc*$^{-/-}$) and wildtype littermates (L-*G6pc*$^{+/+}$) were generated as described previously (14). For tissue collection, mice were sacrificed by cardiac puncture 10 days after the last tamoxifen injection in non-fasted conditions, unless stated otherwise. In separate experiments requiring bile collection, mice were anesthetized by i.p. injection of Hypnorm (10 ml/kg) (Janssen Pharmaceuticals, Tilburg, The Netherlands) and diazepam (10mg/kg) (Actavis, Baarn, The Netherlands), the bile duct was ligated, the gallbladder was cannulated and bile was collected for 30 minutes.

Male L-*FoxO1,3,4* mice C57BL/6 mice were equipped with a permanent catheter in the right jugular vein for infusions and were allowed a recovery period of at least 4 days. Mice were kept in experimental cages during the experiment and the preceding fasting period, allowing frequent collection of tail blood samples. After overnight fasting, mice were infused for 6 hours with S4048 (a generous gift from Sanofi-Aventis, Germany, 5.5 mg/ml PBS with 6% DMSO at 0.135 ml/h) or vehicle. Blood glucose concentrations were measured in tail blood every 30 minutes during the experiment. All experimental procedures were approved by the Institutional Animal Care and Use Committee of the University of Groningen.

Construction, production and *in vivo* transduction of shRNAs using self-complementary AAV vectors

To construct the self-complementary AAV (scAAV) 2/8-U6-shChREBP, the scAAV2-LP1-hFIXco backbone vector was restricted with BamHI and BbsI and the 3493 bp fragment was isolated and ligated. Restriction with BamHI and BbsI removed hFIXco and partially deleted the LP1 promoter and the U6 promoter driving the expression of the construct was cloned into the vector in antisense orientation. shRNA construct directed against ChREBPα/β and scramble construct were ordered as oligonucleotides (shRNA; 5'-aat tcA AAA AAT GTA GTT TGA AGA TGT GGG TCT CGA GAC CCA CAT CTT CAA ACT ACA TC-3' and 3'-ggc caG ATG TAG TTT GAA GAT GTG GGT CTC GAG ACC CAC ATC TTC AAA CTA CAT TTT TT-5', scramble; 5'-aat tcG TTG TAA GTG GAG GTT TAA GTC TCG AGA CTT AAA CCT CCA CTT ACA ACA CCG GT-3' and 3'-ggc caA CCG GTG TTG TAA GTG GAG GTT TAA GTC TCG AGA CTT AAA CCT CCA CTT ACA AC-5') and cloned into the vector using EcoRI and AgeI. Production, purification

and titration of these AAV2/8 viruses encoding the shRNA directed against ChREBPα and ChREBPβ and the scrambled control were performed as described (16). Mice were injected with 5 x 10^{12} virus particles per mouse and sacrificed 30 days after virus administration.

IHH glucose stimulation and transient transfection assays

For glucose stimulation, IHH cells (17) were glucose-deprived in Dulbecco's Modified Eagle Medium (DMEM) (Invitrogen) without glucose, supplemented with 1% penicillin/streptomycin, 0.1% fatty acid-free bovine serum albumin (BSA), 16 mU/mL insulin, 2 mM GlutaMAX (Gibco) and 1 mM glucose for 16 h. Cells were subsequently incubated with low (1 mM) or high (11 mM) glucose concentrations for 24 h. For transient transfection assays, IHH cells were transfected for 48 h using Lipofectamine RNAiMAX Reagent (Invitrogen) according to the manufacturer's protocol with 50 nM ChREBP small interfering RNAs (siChREBP) (18) or control siRNA (#12935-100) (Invitrogen) in Williams E medium containing 2 mM glutamine and supplemented with 2% FCS, 20 mU/mL insulin and 50 nM dexamethasone.

Analytical procedures

Blood glucose was measured using a One Touch Ultra glucose meter (Life-Scan Inc.). Plasma insulin and glucagon were analyzed using commercially available ELISA's (Chrystal Chem and Alpco Diagnostics, respectively). To quantify plasma plant sterols, plasma lipids were extracted according to Folch lipid extraction (19), methanolyzed, silylated and analyzed with gas chromatography. Commercially available kits were used to analyze plasma levels of triglycerides (Roche) and plasma levels of total and free cholesterol (Roche and DiaSys, respectively). Hepatic glycogen and G6P content was determined as previously described (20). Plasma and biliary bile salt composition were quantified using liquid chromatography-mass spectrometry, fecal bile salt composition was quantified using capillary gas chromatography as described (21). The hydrophobicity index of biliary bile acids was calculated according to Heuman (22). Fecal cholesterol and its derivatives were trimethylsilylated with pyridine, N,O-Bis(trimethylsilyl) trifluoroacetaminde and trimethylchlorosilane (ratio 50:50:1) and quantified by gas chromatography.

Gene expression analysis

Total RNA was isolated using TRI-Reagent (Sigma-Aldrich Corp.). cDNA was obtained by reverse transcription and amplified using primers and probes listed in Table S6. mRNA levels were calculated based on a dilution curve, expressed relative to the expression of *36b4* for liver and *18S* for IHH cells, and normalized to their controls.

Targeted proteomics

Targeted proteomics was applied in homogenized liver tissue via the isotopically labeled peptide standards (G6PC; GLGVDLLWTLEK, CYP8B1; VFGYQSVDGDHR, ChREBP; LGFDTLHGLVSTLSAQPSLK, CYP7A1; LSSASLNIR, CYP7B1; YITFVLNPFQYQYVTK, CYP27A1; LYPVVPTNSR, CYP2C70; TDSSLLSR,), containing ^{13}C-labeled lysine/arginine (PolyQuant GmbH, Bad Abbach, Germany) according to the workflow described previously (21). The following alterations were made: lipids were extracted from the liver homogenates with diethyl ether prior to the proteomics workflow and the

concentrations were related to the total peptide content, which was determined by a colorimetric peptide assay after tryptic digestion and SPE cleanup (Thermo Scientific). The concentrations of endogenous peptides were calculated from the known concentration of the standard and expressed in fmol/µg of total peptide and expressed relative to the values in the control group.

Cell reporter assays

CV1 cells (ATCC) were transiently transfected using FuGENE 6 Transfection Reagent (Promega). pCMVS4/ ChREBPα, pCMVS4/ChREBPβ and pCMVS4/Mlx (kind gifts from M. Herman) were shuttled to pcDNA3.1 using cloning PCR. Primers are listed in Table S6. The human or mouse PGL3/Cyp8b1 promoter luciferase reporter (-623/+364 bp and -1582/+115 bp respectively, kind gifts from J. Chiang) or minimal promoter PGL3/ChREBP luciferase reporter (-40/+12) (kind gift from H. Towle) was co-transfected with pcDNA3.1/ChREBPα, pcDNA3.1/ChREBPβ, pcDNA3.1/Mlx, pcDNA3.1/Hnf4α or a combination for 48 h. Cell lysis and luciferase assays were performed using a Dual-Luciferase Reporter Assay System (Promega).

ChIP-qPCR

ChIP analysis was performed as previously described (23) with the following modifications. Before crosslinking with 1% formaldehyde, livers were homogenized in PBS and cross-linked with 0.5M Di(N-succinimidyl) glutarate (DSG) for 45 min at room temperature. Immunoprecipitation of the samples was performed overnight at 4°C with 3 µg ChREBP (Novus), Ac-H4 (Millipore), Ac-H3 (Millipore), HNF4A (Santa Cruz) or normal rabbit IgG antibody (Santa Cruz). DNA was purified using the PCR Clean-up Extraction Kit (Macherey-Nagel), after which qPCR was performed. Primers are listed in Table S7.

Statistics

Statistical analysis was performed using BrightStat software. Differences between two or multiple groups were tested by Mann-Whitney U-test or Kruskal-Wallis H-test followed by post-hoc Conover pairwise comparisons, respectively. P-values <0.001 (***), 0.001 to 0.01 (**), and 0.01 to 0.05 (*) were considered significant. Correlations were analyzed by Spearman's correlations coefficient using SPSS24.0 for Windows software (SPSS, Chicaco, IL, USA).

Results

Hepatic G6P accumulation modifies bile acid synthesis

To establish the selective impact of intracellular glucose on hepatic bile acid synthesis, C57BL/6 mice were infused during 6 hours with S4048, a selective inhibitor of the glucose-6-phosphate transporter SLC37A4, thereby acutely inducing GSD Ib in liver (24). S4048 reduced blood glucose concentrations and increased hepatic G6P and glycogen contents, while glucagon-to-insulin ratios were increased (Table S1). Hepatic mRNA levels of genes involved in bile acid synthesis showed a marked increase in sterol 12α-hydroxylase *(Cyp8b1*) expression, while cholesterol

7α-hydroxylase (*Cyp7a1*) and sterol 27-hydroxylase (*Cyp27a1*) expression were reduced and *Cyp7b1* and *Cyp2c70* expression remained unchanged (Fig. 1A). S4048 infusion did not alter biliary bile acid composition or plasma bile acid levels (Fig. 1B, Fig. S1A). Presumably the timeframe of S4048 infusion is too short to translate into altered bile acid composition: the cycling time of the murine bile acid pool is approximately 4-5 hours and only 5% of biliary bile acids is derived from *de novo* synthesis (25).

Next, we performed similar analyses in mice with sustained hepatic G6P accumulation, i.e., fasted liver-specific *G6pc* knockout (L-*G6pc*$^{-/-}$) mice (14), which exhibited increased glucagon-to-insulin ratios (Table S1). In these animals, hepatic *Cyp8b1* mRNA levels were also strongly elevated while expression of *Cyp7a1, Cyp27a1*, *Cyp7b1* and *Cyp2c70* was significantly lower as compared to L-*G6pc*$^{+/+}$ littermates (Fig. 1C). Altered expression of bile acid synthesis genes in L-*G6pc*$^{-/-}$ mice did translate into a relative increase in CA and CA-derived bile acids (Fig. 1D, Table 1). Similar increases in CA and DCA and concomitant decreases in CDCA and CDCA-derived muricholic acids (MCAs) were observed in plasma and feces from L-*G6pc*$^{-/-}$ mice (Fig. S1B, C, Table S2). Biliary bile acid secretion rates and plasma bile acid concentrations were not different between L-*G6pc*$^{-/-}$ and L-*G6pc*$^{+/+}$ mice (Fig. 1E, Table 1).

Interestingly, hepatic CYP7A1 protein levels, but not *Cyp7a1* mRNA levels, were lower in L-*G6pc*$^{-/-}$ mice as compared to wildtype littermates (Fig. 1F), and hepatic CYP7A1 protein levels positively correlated with blood glucose levels (Fig. 1G). Similar correlations were observed for plasma 7α-hydroxy-4-cholesten-3-one (C4) levels, the product of CYP7A1 and a marker of its activity (26) (Fig. 1G). C4 levels were significantly lower in fasted mice compared to fed mice (median 29.7 *vs.* 54.6 nmol/L, *p*-value 0.022). On the other hand, hepatic CYP8B1 mRNA and protein levels were significantly increased in L-*G6pc*$^{-/-}$ mice irrespective of the feeding state (Fig. 1H).

To assess whether this G6P-dependent modulation of bile acid metabolism is conserved in human hepatocytes, we exposed immortalized human hepatocyte (IHH) cells, that are glucose-responsive (17), to high and low glucose culture media. Next to the expected induction of pyruvate kinase L/R (*PKLR; L-PK*) and apolipoprotein C3 (*APOC3*) mRNA levels, high glucose increased expression of *CYP8B1* as well as of *CYP7A1*, but did not affect *CYP7B1* expression (Fig. S1D). *CYP27A1* is not expressed in IHH cells.

ChREBP mediates the response of bile acid synthesis to hepatic G6P accumulation

To elucidate the mechanism of G6P-dependent control of *Cyp8b1*, we performed S4048 infusions in mice lacking Forkhead Box O (FoxO) 1,3,4 expression in hepatocytes and in mice with reduced hepatic expression of the G6P-sensitive transcription factor Carbohydrate responsive element binding protein (ChREBP), which is activated in GSD Ia and GSD Ib (12,24,27). We confirmed that FoxOs control basal *Cyp8b1* expression (4), and found that the S4048-mediated induction of

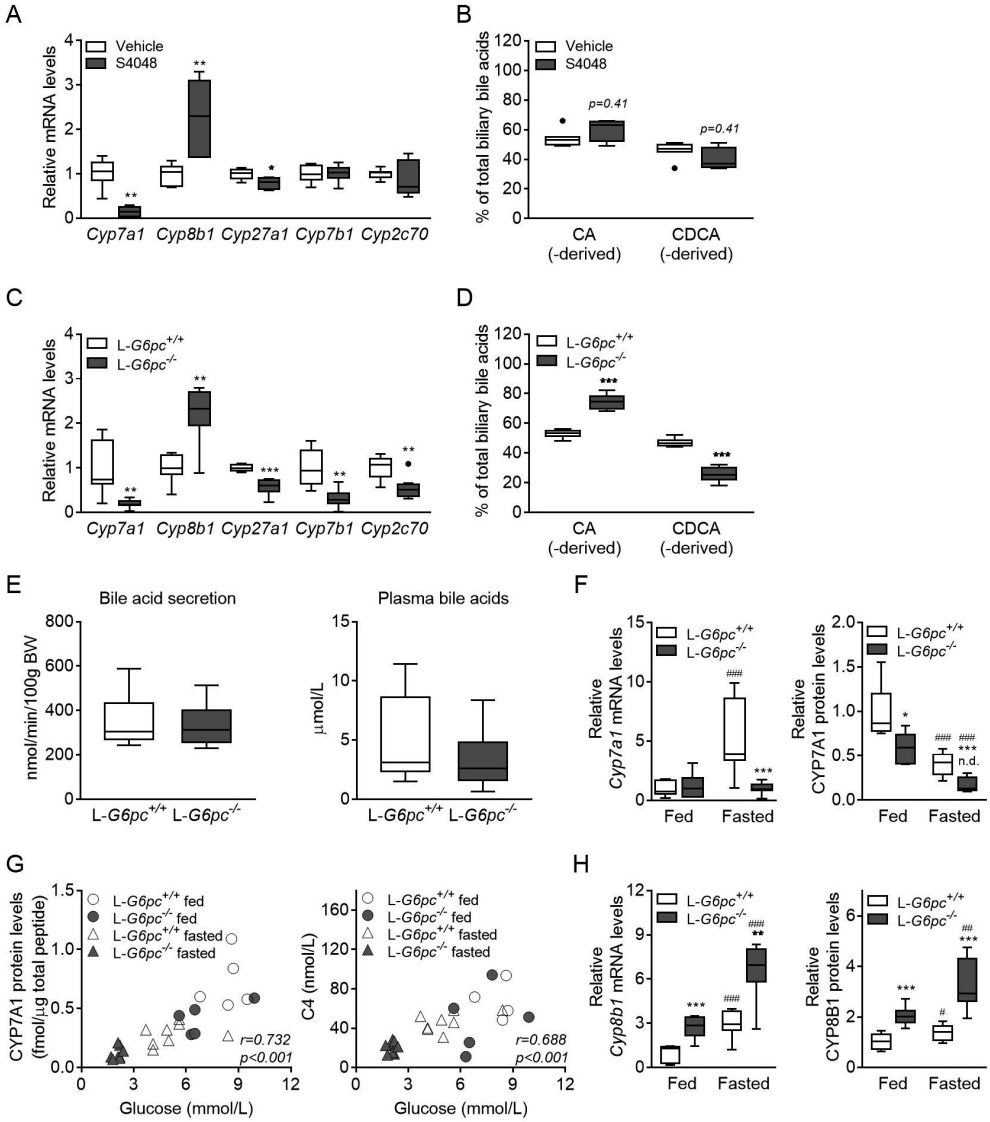

Figure 1. Hepatic G6P accumulation modifies bile acid synthesis. (A) Hepatic mRNA levels of bile acid synthesis genes and (B) Biliary bile acid composition in C57BL/6 mice infused with S4048 or vehicle (n = 7). (C) Hepatic mRNA levels of bile acid synthesis genes, (D) Biliary bile acid secretion, (E) Plasma bile acid levels and (F) Biliary bile acid composition in L-*G6pc*$^{-/-}$ and L-*G6pc*$^{+/+}$ mice (n = 7-8). (G) Correlation between blood glucose levels and hepatic *Cyp7a1* mRNA levels and (H) correlation between blood glucose levels and plasma C4 levels in fasted L-*G6pc*$^{-/-}$ mice and L-*G6pc*$^{+/+}$ mice, and C57BL/6 mice infused with S4048 or vehicle (n = 7-8). Data represent Tukey boxplots. ***p < 0.001, **p <0.01, *p < 0.05. See also Figure S1 and Table S1, S2 and S3.

Cyp8b1 was absent in L-*FoxO1,3,4*$^{-/-}$ mice (Fig. 2A). Interestingly, the induction of *Cyp8b1* upon S4048 infusion was also abolished in mice with reduced hepatic *Chrebpα* and *Chrebpβ* expression (Fig. 2A, Fig. S2B). Similar effects were observed on *Cyp8b1* mRNA and protein levels upon hepatic ChREBP knockdown in L-*G6pc*$^{-/-}$ mice (Fig. 2B, C). The S4048-mediated reduction in *Cyp7a1* expression was comparable in *FoxO1,3,4*$^{+/+}$ and L-*FoxO1,3,4*$^{-/-}$ mice (Fig. S2A). Hepatic mRNA and protein levels of *Cyp7a1* and *Cyp7b1* were induced in response to ChREBP knockdown in L-*G6pc*$^{+/+}$ mice only, while *Cyp27a1* and *Cyp2c70* levels remained unaltered. (Fig. S2C, D). The hepatic expression of *Nr1h4* (*Fxr*), *Nr5a2* (*Lrh-1*), *Hnf4a* (*Hnf4α*), and *Mafg,* established transcriptional regulators of *Cyp8b1*, remained largely unaffected upon hepatic G6P accumulation and were exclusively reduced when ChREBP was knocked down in S4048-treated or L-*G6pc*$^{-/-}$ mice (Fig. S2E, F). Hepatic *Nr0b2* (*Shp*) mRNA levels were lower in both S4048-treated and L-*G6pc*$^{-/-}$ mice, and were further reduced in response to hepatic ChREBP knockdown in L-*G6pc*$^{+/+}$ and L-*G6pc*$^{-/-}$ mice (Fig. S2E, F).

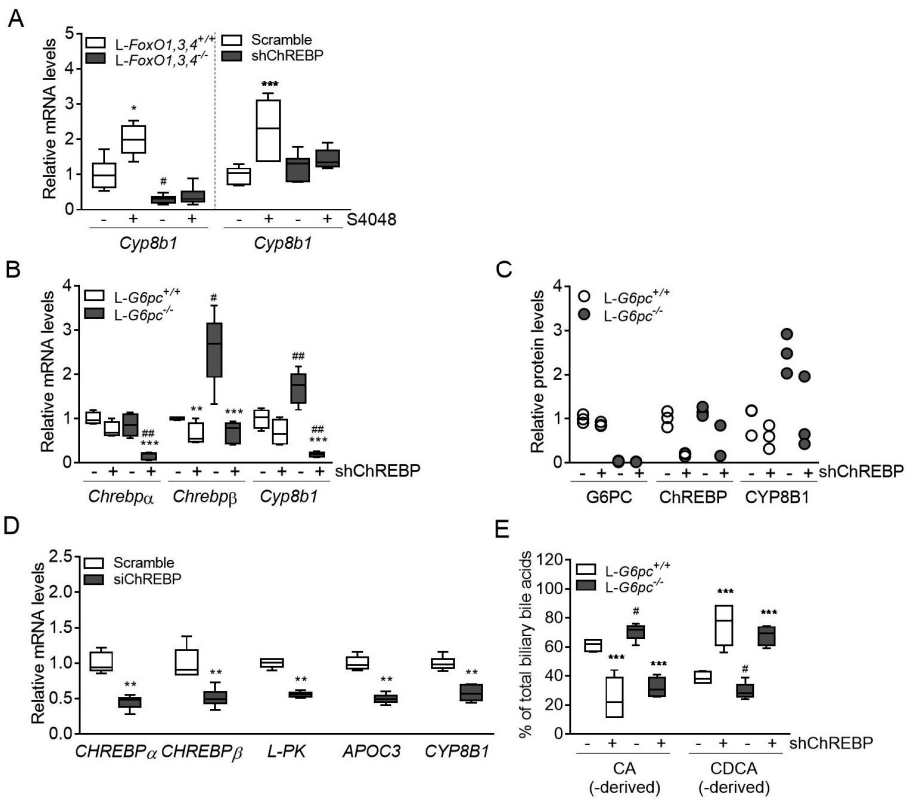

Figure 2. ChREBP mediates the induction of *Cyp8b1* in response to hepatic G6P accumulation. (A) Hepatic mRNA levels of *Cyp8b1* in L-*FoxO1,3,4*$^{-/-}$ and L-*FoxO1,3,4*$^{+/+}$ mice and in C57BL/6 mice treated with either shChREBP or scrambled shRNA, infused with S4048 or vehicle (n = 7-8). (B) Hepatic mRNA levels in L-*G6pc*$^{-/-}$ and L-*G6pc*$^{+/+}$ mice, treated with either shChREBP or scrambled shRNA (n = 4-6). (C) Hepatic protein levels of G6PC, ChREBP and CYP8B1 in L-*G6pc*$^{-/-}$ and L-*G6pc*$^{+/+}$ mice, treated with either shChREBP or scrambled

shRNA (n = 3). (D) mRNA expression in IHH cells transfected with siChREBP or scramble after high (11 mM) glucose exposure for 24 hours (n = 6). (E) Biliary bile acid composition in L-*G6pc*$^{-/-}$ and L-*G6pc*$^{+/+}$ mice treated with either shChREBP or scrambled shRNA (n = 4-5). Data represent Tukey boxplots. ***p < 0.001, **p <0.01, *p < 0.05 indicates significance compared to scrambled shRNA. #p < 0.05 indicates significance compared to wildtype littermates. See also Figure S2 and Table S5.

To establish the contribution of ChREBP to the glucose-mediated *CYP8B1* induction in human hepatocytes, IHH cells were transfected with siChREBP or scrambled ChREBP siRNAs under conditions of high glucose exposure. siChREBP reduced the expression of *CHREBPα*, *CHREBPβ*, the ChREBP target genes *L-PK* and *APOC3*, as well as that of *CYP8B1* by about 50% (Fig. 2D). *CYP7A1* and *CYP7B1* slightly increased upon ChREBP knockdown in IHH cells (Fig. S2G).

Then we evaluated whether the G6P-ChREBP dependent induction of *Cyp8b1* translated into qualitative changes in biliary and plasma bile acids. Hepatic G6P accumulation increased the contribution of biliary CA and DCA and increased plasma CA and DCA levels in L-*G6pc*$^{-/-}$ mice while administration of shChREBP had the opposite effect (Fig. 2E, S2H, Table S3, S4, S5), consistent with the observed decrease in hepatic *Cyp8b1* expression (Fig. 2B, C, S2B). Combined, these data indicate that G6P-ChREBP induce qualitative changes in biliary and plasma bile acid composition *via* the induction of hepatic *Cyp8b1* expression.

ChREBP does not directly regulate hepatic Cyp8b1 transcription

We next investigated whether ChREBP directly regulates Cyp8b1 transcription. Analysis of a hepatic ChREBP ChIP-seq data set (28) indicated potential regulation of Cyp8b1 by ChREBP. Computational analysis revealed three putative ChREBP response elements similar to the ChREBP consensus sequence (CAYGYGnnnnnCRCRTG), and one element with an alternative sequence (GGGGGYGGGC) in the mouse Cyp8b1 promoter (Fig. 3A). Cell reporter assays did not show transactivation of the murine or human *Cyp8b1* promoter by ChREBPα or ChREBPβ, while both *Cyp8b1* reporters used were transactivated by Hnf4α (Fig. 3B) (29), and the minimal *Acaca* (*Acc*) promoter (30) did show ChREBP responsiveness (Fig. 3B). In agreement with these findings, *in vivo* ChIP analysis did not show a strong interaction of ChREBP with the putative response elements in the mouse *Cyp8b1* promoter while S4048 treatment promoted ChREBP recruitment to the *Pklr* (*L-pk*) promoter (Fig. 3A, C) (31). Moreover, HNF4α recruitment to the *Cyp8b1* and *L-pk* promoter regions was not altered upon ChREBP knockdown, indicating that the effect of ChREBP was likely not mediated by increased HNF4α binding to *Cyp8b1* (Fig. S3A). We confirmed that acetylated histone 3 and 4 (H3/4) mainly interacted with the transcribed region of the *Cyp8b1* promoter (Fig. S3B, Fig. 3D) (32). Although we did not observe changes in binding of acetylated H3, the binding of acetylated H4 was reduced under conditions of combined hepatic ChREBP knockdown and G6P accumulation (Fig. 3D). Altogether, these findings demonstrate that the induction of *Cyp8b1* expression by G6P-ChREBP is associated with increased recruitment of acetylated H4, but not of ChREBP, HNF4α or acetylated H3 to the *Cyp8b1* locus.

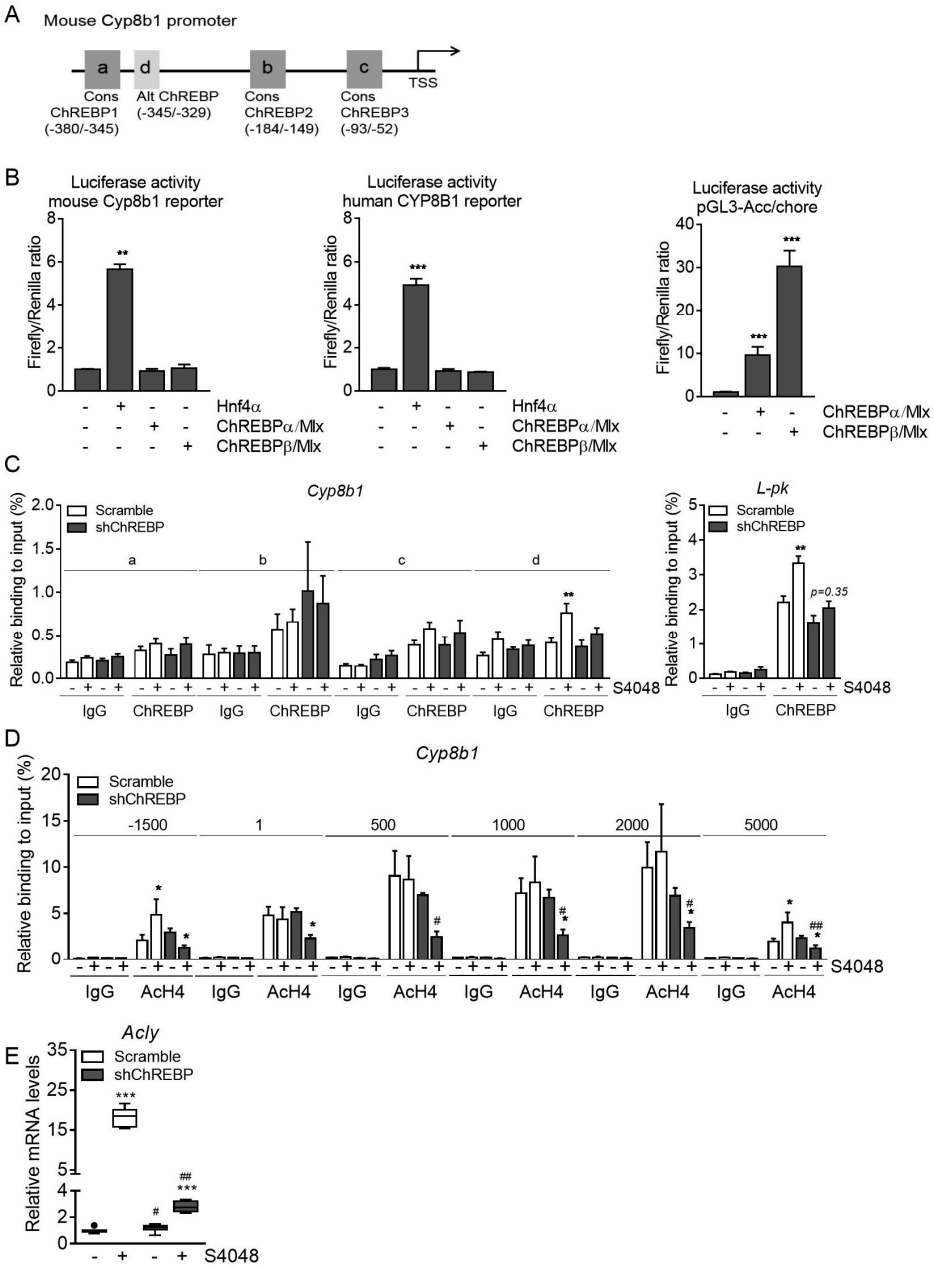

Figure 3. ChREBP does not directly regulate hepatic *Cyp8b1* transcription.
(A) Schematic presentation of putative consensus and alternative ChREBP response elements within the murine *Cyp8b1* promoter. (B) Luciferase activity for the murine and human CYP8B1 promoter reporter and minimal promoter ACC/chore after transfection with Hnf4α, ChREBPα and ChREBPβ plasmids (n = 5-6). (C) In vivo ChIP analysis of the putative ChREBP response elements in the hepatic *Cyp8b1* and *L-pk* gene and (D) of acetylated histone H4 around the hepatic *Cyp8b1* gene in mice treated with either shChREBP or

scrambled shRNA and infused with S4048 or vehicle (n = 7). Data are represented as means ± SEM. ***p < 0.001, **p <0.01, *p < 0.05 indicates significance compared to vehicle controls. ##p < 0.01, #p < 0.05 indicates significance compared to controls treated with scrambled shRNA. See also Figure S3.

G6P-ChREBP increases biliary bile acid hydrophobicity and reduces fecal sterol loss

A shift in the contribution of CA *versus* CDCA-derived bile acids alters the hydrophobicity of the bile acid pool (22) and, in turn, changes the capacity for intestinal lipid solubilization and –uptake (1,7,33–35). The induction of hepatic *Cyp8b1* expression and relative increase in CA and DCA in L-*G6pc*$^{-/-}$ mice (Fig. 1C, D) increased the hydrophobicity index of the biliary bile acids entering the intestine (Fig. 4A) while hepatic ChREBP knockdown reduced this index (Fig. 4B). We confirmed

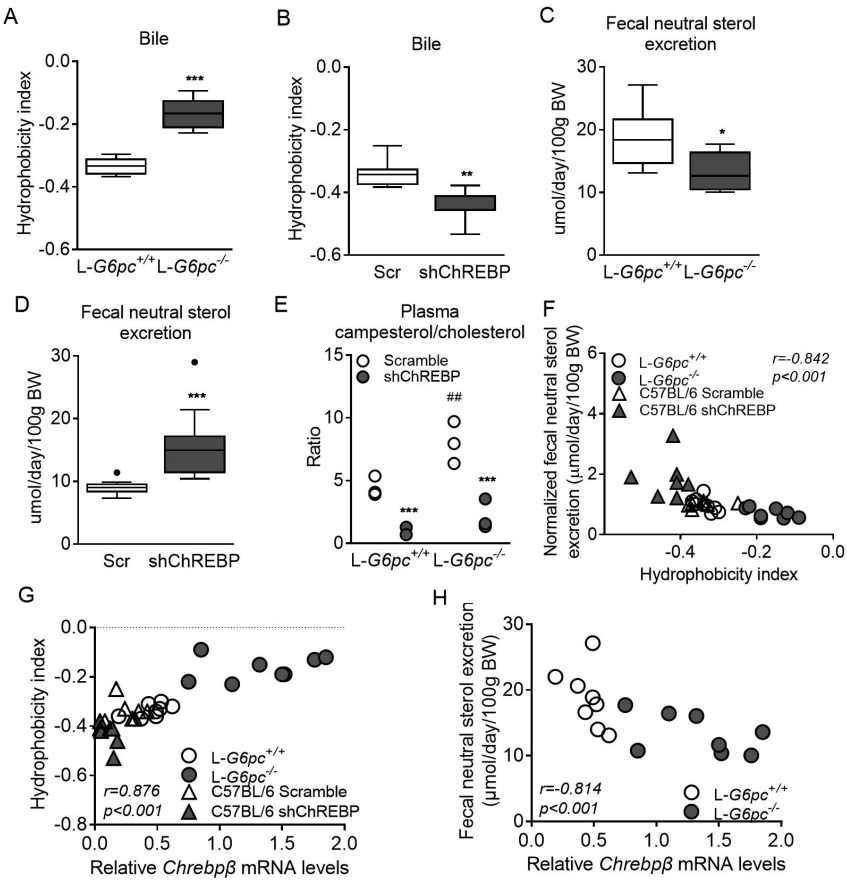

Figure 4. G6P-ChREBP increases bile acid pool hydrophobicity and reduces fecal sterol loss. (A) Biliary bile hydrophobicity index of L-*G6pc*$^{-/-}$ and L-*G6pc*$^{+/+}$ mice and (B) mice treated with either shChREBP or scrambled (scr) shRNA (n = 7-8). (C) Fecal neutral sterol excretion of L-*G6pc*$^{-/-}$ and L-*G6pc*$^{+/+}$ mice (n = 8) and (D) mice treated with either shChREBP or scrambled shRNA (n = 14). (E) Plasma campesterol/cholesterol ratios in L-*G6pc*$^{-/-}$ and L-*G6pc*$^{+/+}$ mice treated with either shChREBP or scrambled shRNA (n = 3). (F) Correlation between bile

hydrophobicity index and normalized fecal neutral sterol excretion and between (G) ChREBPβ mRNA levels and bile hydrophobicity index in L-*G6pc*$^{-/-}$ and L-*G6pc*$^{+/+}$ mice, and mice treated with either shChREBP or scrambled shRNA (n = 7-8). (H) Correlation between ChREBPβ mRNA levels and fecal neutral sterol excretion in L-*G6pc*$^{-/-}$ and L-*G6pc*$^{+/+}$ mice (n = 8). Data represent Tukey boxplots. ***p < 0.001, **p <0.01, *p < 0.05 indicates significance compared to wildtype littermates or controls treated with scrambled shRNA. ##p < 0.01 indicates significance compared wildtype littermates. See also Figure S3.4.

that hepatic *Cyp8b1* expression was positively correlated to biliary bile acid hydrophobicity in L-*G6pc*$^{-/-}$ mice (36) (Fig. S4A) and hypothesized that altered hydrophobicity in response to G6P-ChREBP-CYP8B1 signaling impacts intestinal sterol absorption (33,35). Hepatic *Cyp8b1* expression indeed negatively correlated with fecal neutral sterol excretion (35) (Fig. S4B). Fecal neutral sterol excretion was reduced in L-*G6pc*$^{-/-}$ mice (Fig. 4C, Fig. S4C) and, as expected, increased upon hepatic ChREBP knockdown (Fig. 4D, Fig. S4C). The plasma campesterol/cholesterol ratio, a marker of intestinal cholesterol absorption (37), showed similar patterns (Fig. 4E). Bile hydrophobicity and fecal neutral sterol excretion were found to be negatively correlated (Fig. 4F) and hepatic *Chrebpβ* mRNA expression showed a positive correlation to hydrophobicity index (Fig. 4G) while it was negatively correlated with fecal neutral sterol excretion (Fig 4H). Fecal energy and -fatty acid excretion remained unchanged in response to hepatic G6P accumulation or ChREBP knockdown (Fig. S4D, E).

Table 1. Bile characteristics in chow-fed male L-*G6pc*$^{-/-}$ mice and wildtype littermates.

	L-*G6pc*$^{+/+}$	L-*G6pc*$^{-/-}$	
	Median (Range)	Median (Range)	*p*-value
Body weight (g)	28.4 (21.5 - 29.9)	27.5 (25.3 - 32.5)	0.645
Bile flow (µL/min/100g BW)	12.2 (8.5 - 15.0)	14.6 (12.3 - 18.5)	**0.021**
Bile acid secretion (nmol/min/100g BW)	305.1 (244.3 - 587.5)	313.3 (229.7 - 514.5)	0.878
Phospholipid secretion (nmol/min/100g BW)	81.1 (75.3 - 164.9)	109.7 (93.2 - 159.4)	**0.038**
Cholesterol secretion (nmol/min/100g BW)	11.6 (9.5 - 17.1)	12.7 (10.7 - 18.6)	0.161
Bile acid species secretion (nmol/min/100g BW)			
CA	3.88 (1.18 - 7.15)	3.13 (0.86 - 6.07)	0.959
GCA	0.58 (0.21 - 1.21)	0.45 (0.31 - 0.75)	0.279
TCA	150.17 (124.91 - 292.16)	226.74 (164.34 - 344.06)	**0.028**
TUDCA	5.11 (3.86 - 11.26)	3.92 (2.58 - 7.33)	0.105
TCDCA	2.01 (1.61 - 4.98)	2.63 (1.32 - 5.84)	0.645
TDCA	6.59 (3.40 - 13.85)	9.18 (2.14 - 15.74)	0.442
THDCA	2.27 (0.56 - 3.89)	1.40 (0.79 - 2.17)	0.279
α-MCA	0.40 (0.14 - 1.48)	0.31 (0 - 1.18)	0.279
Tα-MCA	11.37 (9.18 - 36.33)	12.48 (6.9 - 29.22)	0.878
β-MCA	2.65 (0.52 - 5.13)	0.42 (0 - 1.17)	**0.007**
Tβ-MCA	117.01 (87.53 - 212.07)	52.38 (30.24 - 117.05)	**0.002**
ω-MCA	2.61 (0.84 - 7.07)	0.84 (0.38 - 1.78)	**0.005**

Discussion

In the current study we characterized an important regulatory role of glucose, independent of insulin, in the control of hepatic bile acid synthesis. Using the monogenetic disease GSD I as a model to establish the contribution of intrahepatic glucose, we are the first to show that G6P controls hepatic bile acid synthesis *via* ChREBP-dependent induction of *Cyp8b1* in mice. G6P-ChREBP signaling increases the relative abundance of CA-derived bile acids and induces physiologically relevant shifts in bile composition. We confirmed that the human *CYP8B1* gene is regulated *via* a similar mechanism. Importantly, our work also demonstrates the physiological relevance of this novel regulatory mechanism: the G6P-ChREBP-dependent change in bile acid hydrophobicity in mice associates with reduced fecal neutral sterol loss and lower plasma campesterol/cholesterol ratios, compatible with enhanced intestinal cholesterol absorption.

Besides the novel G6P-dependent regulation of CYP8B1, we found that hepatic levels of CYP7A1 protein, the supposedly rate-controlling enzyme in bile acid synthesis (6), as well as the plasma concentrations of its product C4 correlated with circulating glucose levels. Several studies have reported altered hepatic *Cyp7a1* mRNA expression in response to changes in hepatic glucose availability (9,38). We and others have shown that type 1 and type 2 diabetic rodents exhibit increased hepatic expression of *Cyp7a1* (38) and an enlarged bile acid pool (39,40). On the other hand, prolonged fasting decreases hepatic *Cyp7a1* mRNA expression in mice, with a concomitant reduction of the total bile acid pool size (38), consistent with our finding that hypoglycemia is associated with lower hepatic CYP7A1 protein levels. These data indicate that the blood glucose level regulates CYP7A1 protein levels independently of hepatic G6P accumulation, possibly via its effect on the insulin-to-glucagon ratio (8,9), but independently of hepatic FOXO1,3,4 expression (Fig. S2A).

We thus show that hepatic *Cyp7a1* expression is partly controlled by circulating glucose levels, while intrahepatic glucose (G6P) appears to be the major regulator of *Cyp8b1* expression. Importantly, the ChREBP-dependent induction of *Cyp8b1* was rapid and cell-autonomous, as we found a similar regulation within 6 hours in mouse liver and in 24 hour glucose-stimulated human hepatocytes. Previous studies have reported an induction of *Cyp8b1* by glucose *in vitro* (9) and an insulin-mediated suppression of the gene *in vivo* (2,4). We now show, in insulin-sensitive mice, that the glucose-mediated induction of *Cyp8b1* requires hepatic ChREBP. The exact molecular mechanism by which G6P-ChREBP controls *Cyp8b1* transcription remains elusive, as we could not demonstrate direct transcriptional regulation. We did, however, show that recruitment of acetylated H4 was reduced under conditions of combined hepatic ChREBP knockdown and G6P accumulation (Fig. 3D), indicating reduced transcriptional activity under these conditions. ChREBP is a key determinant of glycolysis and a direct transcriptional regulator of ATP-citrate lyase (41), the essential enzyme for glucose-induced histone acetylation on the *Cyp7a1* locus (9,42). It is therefore conceivable that hepatic ChREBP knockdown limits acetyl-CoA availability from glycolysis for histone acetylation. We also observed that FoxO1/3/4

expression was essential for the G6P-dependent induction of *Cyp8b1* (Fig. 2A). Considering that L-*G6pc*$^{-/-}$ mice have increased hepatic FoxO3a acetylation (43), hepatic G6P accumulation and/or ChREBP knockdown potentially regulate hepatic Cyp8b1 expression *via* FoxO3a acetylation. Altogether, we hypothesize that G6P-ChREBP signaling may alter the activity of a second transcription factor such as FoxO1/3/4 and/or HNF4α (44,45), hence indirectly regulating *Cyp8b1* expression.

Hydrophobic bile acids effectively promote the absorption of dietary lipids and sterols (33–35) while a more hydrophilic bile acid pool is associated with enhanced intestinal cholesterol excretion (21). Our data strongly suggest that ChREBP activity contributes to cholesterol homeostasis in mice *via* its effect on CYP8B1 and, hence, on bile acid composition. The ChREBP-mediated increase in CA and decrease in β-MCA synthesis resulted in more hydrophobic bile that was paralleled by reduced fecal neutral sterol excretion. Because dietary cholesterol intake (data not shown), biliary cholesterol excretion (Table 1) and jejunal and ileal mRNA expression of *Npc1l1*, *Abcg5*, *Abcg8* and *Acat2* (data not shown) were similar in L-*G6pc*$^{-/-}$ mice and wildtype littermates, the reduction in neutral sterol excretion is most likely related to enhanced fractional cholesterol absorption as a consequence of the more hydrophobic bile acid pool in L-*G6pc*$^{-/-}$ mice. We also show that normalization of bile composition upon hepatic ChREBP knockdown reverses reduced fecal neutral sterol excretion, consistent with the phenotype of *Cyp8b1*$^{-/-}$ mice and with the effect of *Cyp8b1* inhibition in mice (33,35,46). However, in contrast to what was reported for *Cyp8b1*$^{-/-}$ mice fed a high-fat diet (33,35), fecal fatty acid and energy loss remained unaltered in the current study. In accordance with our findings, *Cyp8b1* heterozygous knockout mice displaying an intermediate phenotype with regard to bile acid pool composition also did not present changes in fecal calorie loss (33). The absence of a change in fecal excretion of non-sterol dietary fat could furthermore be due to the relatively low fat content of the chow diet used, the high efficiency of intestinal fatty acid absorption under normal conditions (47), and the fact that intestinal sterol absorption shows a larger dependency on bile acid hydrophobicity as compared to dietary fatty acids (34). Therefore, we conclude that activation of the hepatic G6P-ChREBP-CYP8B1 axis selectively reduces fecal cholesterol excretion in chow-fed mice.

A major difference in bile acid metabolism between mouse and human is the presence of MCAs in murine bile, due to rodent-specific C6-hydroxylation (48). As MCAs are very hydrophilic (22), the human bile acid pool is more hydrophobic as compared to mice. The G6P-ChREBP-mediated induction of *Cyp8b1*, promoting CA synthesis at the expense of dihydroxylated CDCA, would result in a more hydrophilic rather than a more hydrophobic bile acid pool in humans, with a potentially opposite effect on intestinal cholesterol absorption. There are no reports focusing on disturbed bile acid metabolism in GDS Ia patients, yet it is well-known that bile acid metabolism is perturbed in type 2 diabetes (2,4,5). Although deviations in blood glucose are opposite in GSD Ia and diabetes, intrahepatic glucose metabolism is enhanced in both diseases and the hepatic phenotypes are very similar, rendering GSD Ia a ‘model disease’ for diabetic liver disease (10–15). Type 2 diabetic mice exhibit elevated hepatic *Cyp8b1* expression and a corresponding increase in

12-hydroxylated bile acids (4,40), which has been attributed to insulin resistance and consequent FOXO activation (4). As hepatic ChREBP is also activated in type 2 diabetic mice and humans (49,50), increased G6P-ChREBP signaling potentially contributes to perturbed bile acid metabolism in type 2 diabetes. Therefore, our current data underscore the need to establish the impact of intrahepatic G6P-ChREBP signaling on bile acid pool composition in mice with a humanized bile acid pool (48) and GSD I patients, as well as its contribution to perturbed bile acid metabolism in type 2 diabetes.

In conclusion, we present a novel mechanism by which intracellular glucose controls hepatic bile acid synthesis and intestinal cholesterol handling. The G6P-ChREBP-CYP8B1 signaling cascade that we have identified likely contributes to altered bile acid metabolism and its (patho)physiological consequences in conditions coinciding with excessive intrahepatic glucose signaling such as GSD I and type 2 diabetes.

Acknowledgements

We thank A. Jurdinski, R. Havinga, T. Boer, M. Koehorst, R. Boverhof, Y. van der Veen, K. Tholen, C. van der Leij, S.X. Lee and Z. Unal for excellent technical assistance. We are thankful for receiving plasmids from M. Herman (pcDNA3.1/ChREBPα, pcDNA3.1/ChREBPβ, pcDNA3.1/Mlx, pcDNA3.1/Hnf4α), H. Towle (minimal promoter PGL3/ChREBP luciferase reporter) and J. Chiang (human and mouse PGL3/Cyp8b1 promoter luciferase reporters). We thank A. Herling and D. Schmoll (Sanofi) for providing S4048 and L. Chan for sharing the ChREBP ChIP-seq data set.

References

1. Lefebvre P, Cariou B, Lien F, Kuipers F, Staels B. Role of Bile Acids and Bile Acid Receptors in Metabolic Regulation. Physiol. Rev. 2009;89:147–91.
2. Haeusler RA, Astiarraga B, Camastra S, Accili D, Ferrannini E. Human insulin resistance is associated with increased plasma levels of 12α-hydroxylated bile acids. Diabetes. 2013;62:4184–91.
3. Bennion LJ, Grundy SM. Effects of Diabetes Mellitus on Cholesterol Metabolism in Man. N. Engl. J. Med. 1977;296:1365–1371.
4. Haeusler RA, Pratt-Hyatt M, Welch CL, Klaassen CD, Accili D. Impaired generation of 12-hydroxylated bile acids links hepatic insulin signaling with dyslipidemia. Cell Metab. 2012;15:65–74.
5. Brufau G, Stellaard F, Prado K, Bloks VW, Jonkers E, Boverhof R, et al. Improved glycemic control with colesevelam treatment in patients with type 2 diabetes is not directly associated with changes in bile acid metabolism. Hepatology. 2010;52:1455–64.
6. Chiang JYL. Bile acids: regulation of synthesis. J. Lipid Res. 2009;50:1955–66.
7. Gälman C, Angelin B, Rudling M. Bile acid synthesis in humans has a rapid diurnal variation that is asynchronous with cholesterol synthesis. Gastroenterology. 2005;129:1445–53.
8. Li T, Kong X, Owsley E, Ellis E, Strom S, Chiang JYL. Insulin Regulation of Cholesterol 7α-Hydroxylase Expression in Human Hepatocytes. J. Biol. Chem. 2006;281:28745–28754.
9. Li T, Chanda D, Zhang Y, Choi H-S, Chiang JYL. Glucose stimulates cholesterol 7alpha-hydroxylase gene transcription in human hepatocytes. J. Lipid Res. 2010;51:832–42.
10. Ishida H, Yamashita C, Kuruta Y, Yoshida Y, Noshiro M. Insulin Is a Dominant Suppressor of Sterol 12α-Hydroxylase P450 (CYP8B) Expression in Rat Liver: Possible Role of Insulin in Circadian Rhythm of CYP8B. J. Biochem. 2000;127:57–64.
11. Bandsma RHJ, Grefhorst A, van Dijk TH, van der Sluijs FH, Hammer A, Reijngoud D-J, et al. Enhanced glucose cycling and suppressed de novo synthesis of glucose-6-phosphate result in a net unchanged hepatic glucose output in ob/ob mice. Diabetologia. 2004;47:2022–2031.
12. Oosterveer MH, Schoonjans K. Hepatic glucose sensing and integrative pathways in the liver. Cell. Mol. Life Sci. 2014;71:1453–1467.
13. Chou JY, Mansfield BC. Mutations in the glucose-6-phosphatase-alpha (G6PC) gene that cause type Ia glycogen storage disease. Hum. Mutat. 2008;29:921–930.
14. Mutel E, Abdul-Wahed A, Ramamonjisoa N, Stefanutti A, Houberdon I, Cavassila S, et al. Targeted deletion of liver glucose-6 phosphatase mimics glycogen storage disease type 1a including development of multiple adenomas. J. Hepatol. 2011;54:529–537.
15. Haeusler RA, Kaestner KH, Accili D. FoxOs function synergistically to promote glucose production. J. Biol. Chem. 2010;285:35245–8.
16. Hermens WTJMC, Brake O Ter, Dijkhuizen PA, Sonnemans MAF, Grimm D, Kleinschmidt JA, et al. Purification of Recombinant Adeno-Associated Virus by Iodixanol Gradient Ultracentrifugation Allows Rapid and Reproducible Preparation of Vector Stocks for Gene Transfer in the Nervous System. Hum. Gene Ther. 1999;10:1885–1891.
17. Samanez CH, Caron S, Briand O, Dehondt H, Duplan I, Kuipers F, et al. The human hepatocyte cell lines IHH and HepaRG: models to study glucose, lipid and lipoprotein metabolism. Arch. Physiol. Biochem. 2012;118:102–11.
18. Tong X, Zhao F, Mancuso A, Gruber JJ, Thompson CB. The glucose-responsive

transcription factor ChREBP contributes to glucose-dependent anabolic synthesis and cell proliferation. Proc. Natl. Acad. Sci. U. S. A. 2009;106:21660–5.
19. Folch J, Lees M, Sloane GH. A Simple Method for the Isolation and Purification of Total Lipids from Animal Tissues. J. Biol. Chem. 1957;266:497–509.
20. Bergmeyer HU. Methods of enzymatic analysis [Internet]. Weinheim Germany: Verlag Chemie; 1974.
21. de Boer JF, Schonewille M, Boesjes M, Wolters H, Bloks VW, Bos T, et al. Intestinal Farnesoid X Receptor Controls Transintestinal Cholesterol Excretion in Mice. Gastroenterology. 2017;152:1126–1138.e6.
22. Heuman DM. Quantitative estimation of the hydrophilic- hydrophobic balance of mixed bile salt solutions. J. Lipid Res. 1989;30:719–30.
23. Duggavathi R, Volle DH, Mataki C, Antal MC, Messaddeq N, Auwerx J, et al. Liver receptor homolog 1 is essential for ovulation. Genes Dev. 2008;22:1871–6.
24. Grefhorst A, Schreurs M, Oosterveer MH, Cortés VA, Havinga R, Herling AW, et al. Carbohydrate-response-element-binding protein (ChREBP) and not the liver X receptor α (LXRα) mediates elevated hepatic lipogenic gene expression in a mouse model of glycogen storage disease type 1. Biochem. J. 2010;432:249–54.
25. Kok T, Hulzebos C V, Wolters H, Havinga R, Agellon LB, Stellaard F, et al. Enterohepatic circulation of bile salts in farnesoid X receptor-deficient mice: efficient intestinal bile salt absorption in the absence of ileal bile acid-binding protein. J. Biol. Chem. 2003;278:41930–7.
26. Gälman C, Arvidsson I, Angelin B, Rudling M. Monitoring hepatic cholesterol 7alpha-hydroxylase activity by assay of the stable bile acid intermediate 7alpha-hydroxy-4-cholesten-3-one in peripheral blood. J. Lipid Res. 2003;44:859–66.
27. Abdul-Wahed A, Gautier-Stein A, Casteras S, Soty M, Roussel D, Romestaing C, et al. A link between hepatic glucose production and peripheral energy metabolism via hepatokines. Mol. Metab. 2014;3:531–543.
28. Poungvarin N, Chang B, Imamura M, Chen J, Moolsuwan K, Sae-Lee C, et al. Genome-Wide Analysis of ChREBP Binding Sites on Male Mouse Liver and White Adipose Chromatin. Endocrinology. 2015;156:1982–94.
29. Inoue Y, Yu A-M, Yim SH, Ma X, Krausz KW, Inoue J, et al. Regulation of bile acid biosynthesis by hepatocyte nuclear factor 4alpha. J. Lipid Res. 2006;47:215–27.
30. O'Callaghan BL, Koo SH, Wu Y, Freake HC, Towle HC. Glucose regulation of the acetyl-CoA carboxylase promoter PI in rat hepatocytes. J. Biol. Chem. 2001;276:16033–9.
31. Hasegawa J, Osatomi K, Wu RF, Uyeda K. A novel factor binding to the glucose response elements of liver pyruvate kinase and fatty acid synthase genes. J. Biol. Chem. 1999;274:1100–7.
32. Yamada A, Honma K, Mochizuki K, Goda T. BRD4 regulates fructose-inducible lipid accumulation-related genes in the mouse liver. Metabolism. 2016;65:1478–1488.
33. Bertaggia E, Jensen KK, Castro-Perez J, Xu Y, Di Paolo G, Chan RB, et al. Cyp8b1 ablation prevents Western diet-induced weight gain and hepatic steatosis because of impaired fat absorption. Am. J. Physiol. Endocrinol. Metab. 2017;313:E121–E133.
34. Wang DQ-H, Tazuma S, Cohen DE, Carey MC. Feeding natural hydrophilic bile acids inhibits intestinal cholesterol absorption: studies in the gallstone-susceptible mouse. Am. J. Physiol. Gastrointest. Liver Physiol. 2003;285:G494-502.
35. Bonde Y, Eggertsen G, Rudling M. Mice Abundant in Muricholic Bile Acids Show Resistance to Dietary Induced Steatosis, Weight Gain, and to Impaired Glucose Metabolism. PLoS One. 2016;11:e0147772.
36. Pandak WM, Bohdan P, Franklund C, Mallonee DH, Eggertsen G, Bjorkhem I, et al. Expression of sterol 12α-hydroxylase alters bile acid pool composition in primary rat

hepatocytes and in vivo. Gastroenterology. 2001;120:1801–1809.
37. Stellaard F, von Bergmann K, Sudhop T, Lütjohann D. The value of surrogate markers to monitor cholesterol absorption, synthesis and bioconversion to bile acids under lipid lowering therapies. J. Steroid Biochem. Mol. Biol. 2017;169:111–122.
38. Li T, Francl JM, Boehme S, Ochoa A, Zhang Y, Klaassen CD, et al. Glucose and insulin induction of bile acid synthesis: mechanisms and implication in diabetes and obesity. J. Biol. Chem. 2012;287:1861–73.
39. Van Waarde WM, Verkade HJ, Wolters H, Havinga R, Baller J, Bloks V, et al. Differential effects of streptozotocin-induced diabetes on expression of hepatic ABC-transporters in rats. Gastroenterology. 2002;122:1842–1852.
40. Herrema H, Meissner M, van Dijk TH, Brufau G, Boverhof R, Oosterveer MH, et al. Bile salt sequestration induces hepatic *de novo* lipogenesis through farnesoid X receptor- and liver X receptorα-controlled metabolic pathways in mice. Hepatology. 2010;51:806–816.
41. Sae-Lee C, Moolsuwan K, Chan L, Poungvarin N. ChREBP Regulates Itself and Metabolic Genes Implicated in Lipid Accumulation in β-Cell Line. PLoS One. 2016;11:e0147411.
42. Wellen KE, Hatzivassiliou G, Sachdeva UM, Bui T V, Cross JR, Thompson CB. ATP-citrate lyase links cellular metabolism to histone acetylation. Science. 2009;324:1076–80.
43. Cho J-H, Kim G-Y, Pan C-J, Anduaga J, Choi E-J, Mansfield BC, et al. Downregulation of SIRT1 signaling underlies hepatic autophagy impairment in glycogen storage disease type Ia. PLoS Genet. 2017;13:e1006819.
44. Housley MP, Rodgers JT, Udeshi ND, Kelly TJ, Shabanowitz J, Hunt DF, et al. *O* -GlcNAc Regulates FoxO Activation in Response to Glucose. J. Biol. Chem. 2008;283:16283–16292.
45. Yokoyama A, Katsura S, Ito R, Hashiba W, Sekine H, Fujiki R, et al. Multiple post-translational modifications in hepatocyte nuclear factor 4α. Biochem. Biophys. Res. Commun. 2011;410:749–753.
46. Chevre R, Trigueros-Motos L, Castaño D, Chua T, Corlia M, Patankar J V, et al. Therapeutic modulation of the bile acid pool by Cyp8b1 knockdown protects against nonalcoholic fatty liver disease in mice. FASEB J. 2018;32:3792–3802.
47. Werner A, Minich DM, Havinga R, Bloks V, Van Goor H, Kuipers F, et al. Fat malabsorption in essential fatty acid-deficient mice is not due to impaired bile formation. Am J Physiol Gastrointest Liver Physiol. 2002;283:900–908.
48. Takahashi S, Fukami T, Masuo Y, Brocker CN, Xie C, Krausz KW, et al. Cyp2c70 is responsible for the species difference in bile acid metabolism between mice and humans. J. Lipid Res. 2016;57:2130–2137.
49. Dentin R, Benhamed F, Hainault I, Fauveau VR, Foufelle F, Dyck JRB, et al. Liver-Specific Inhibition of ChREBP Improves Hepatic Steatosis and Insulin Resistance in ob/ob Mice. Diabetes. 2006;55:2159–2170.
50. Kursawe R, Caprio S, Giannini C, Narayan D, Lin A, D'Adamo E, et al. Decreased transcription of ChREBP-α/β isoforms in abdominal subcutaneous adipose tissue of obese adolescents with prediabetes or early type 2 diabetes: associations with insulin resistance and hyperglycemia. Diabetes. 2013;62:837–44.

Supplementary Figures

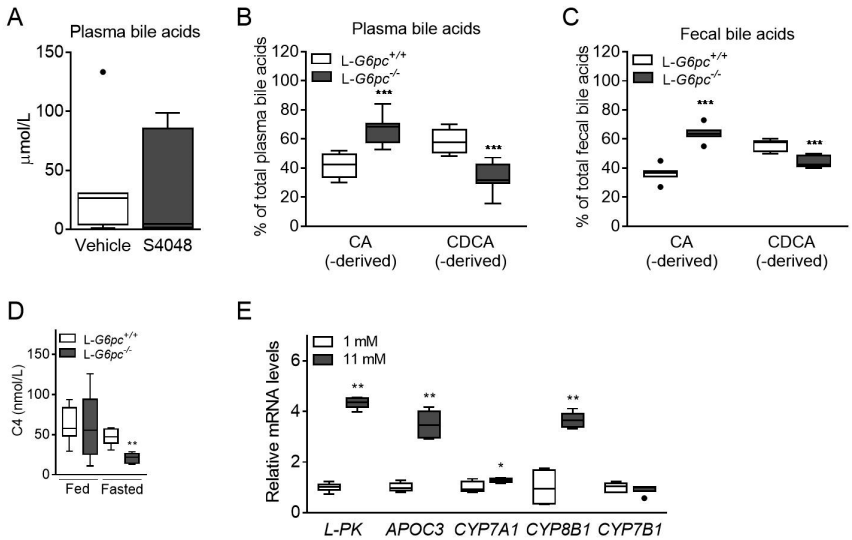

Figure S1. (A) Plasma bile acid levels in C57BL/6 mice infused with S4048 or vehicle (n = 7). (B) Plasma and (C) Fecal bile acid composition in L-*G6pc*$^{-/-}$ and L-*G6pc*$^{+/+}$ mice (n = 7-8). (D) Plasma C4 levels in L-*G6pc*$^{-/-}$ and L-*G6pc*$^{+/+}$ mice in either fed state or after an overnight fast (n = 7-8). (E) mRNA expression in IHH cells after low (1 mM) or high (11 mM) glucose exposure for 24 hours (n = 6). Data represent Tukey boxplots. ***p < 0.001, ** p < 0.01 indicates significance compared to wildtype littermates or low glucose exposure.

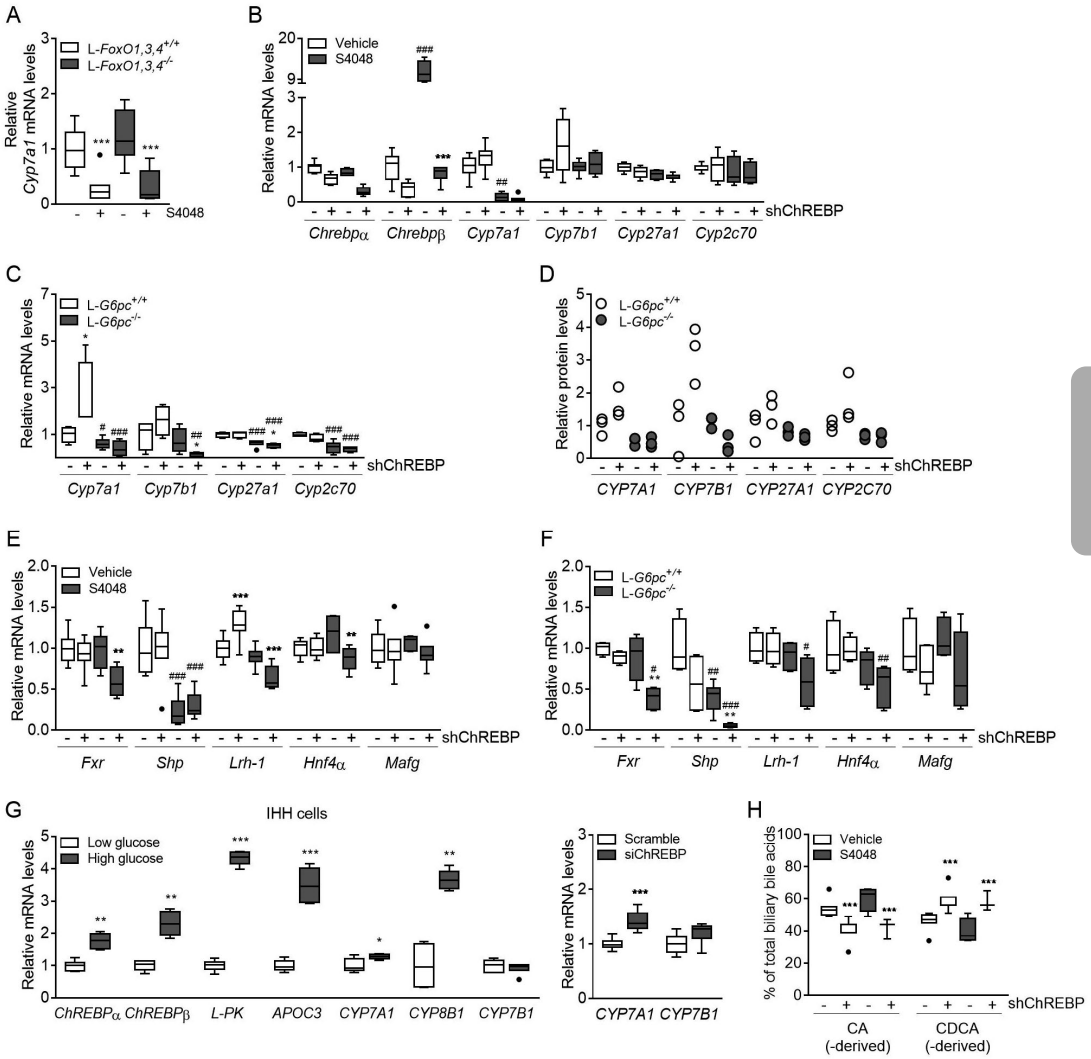

Figure S2. (A) Hepatic *Cyp7a1* mRNA levels in L-*FoxO1,3,4*$^{+/+}$ and L-*FoxO1,3,4*$^{-/-}$ mice treated with S4048 or vehicle (n = 7-9). (B) Hepatic mRNA levels in C57BL/6 mice treated with either shChREBP or scrambled shRNA and infused with S4048 or vehicle (n = 6-7). (C) Hepatic mRNA and (D) Protein levels of bile acid synthesis enzymes in L-*G6pc*$^{+/+}$ and L-*G6pc*$^{-/-}$ mice treated with either shChREBP or scrambled shRNA (n = 3-6). Hepatic mRNA levels of transcriptional regulators of *Cyp8b1* in (E) S4048 or vehicle-infused C57BL/6 mice or (F) L-*G6pc*$^{-/-}$ and L-*G6pc*$^{+/+}$ mice treated with either shChREBP or scrambled shRNA (n = 4-7). (G) mRNA expression in IHH cells exposed to low glucose (1 mM) or high glucose (11 mM) or transfected with siChREBP or scramble after high glucose exposure for 24 hours (n = 6). (H) Biliary bile acid composition in mice treated with either shChREBP or scrambled shRNA and infused with S4048 or vehicle (n = 3-7). Data represent Tukey boxplots. ***p < 0.001, **p < 0.01, *p < 0.05 indicates significance compared to scrambled shRNA. ###p < 0.001, ##p < 0.01, #p < 0.05 indicates significance compared to vehicle controls or wildtype littermates.

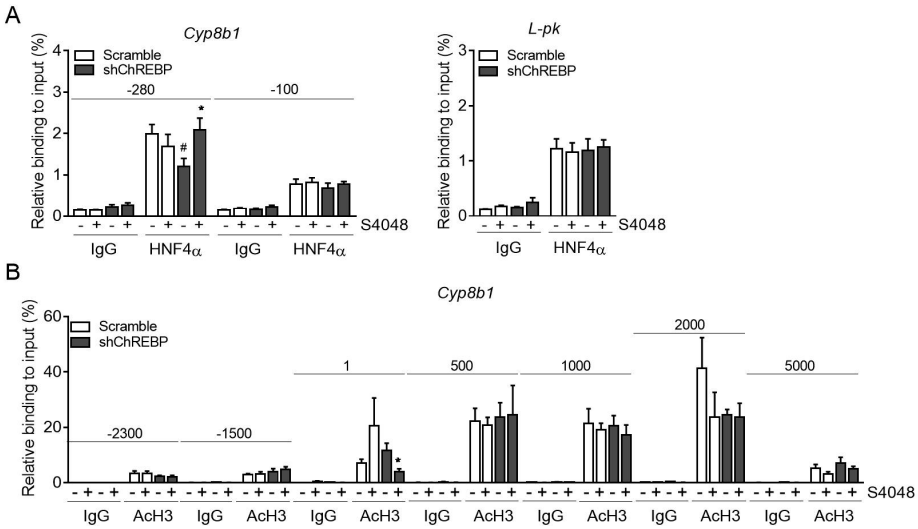

Figure S3. (A) *In vivo* ChIP analysis of the putative HNF4 response elements of the hepatic *Cyp8b1* and *L-pk* gene and (B) acetylated histone H3 at the hepatic *Cyp8b1* gene locus in mice treated with either shChREBP or scrambled shRNA and infused with S4048 or vehicle (n = 4-7). Data represent means ± SEM. *p < 0.05 indicates significance compared to scrambled shRNA. #p < 0.05 indicates significance compared to vehicle controls.

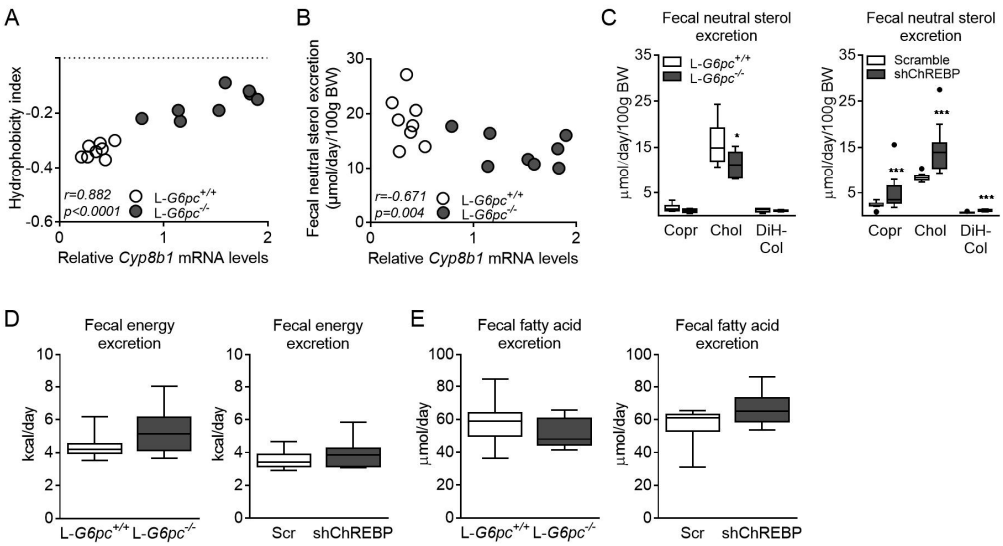

Figure S4. (A) Correlation between *Cyp8b1* mRNA levels and bile hydrophobicity index and (B) correlation between *Cyp8b1* mRNA levels and fecal neutral sterol excretion in L-*G6pc*$^{-/-}$ and L-*G6pc*$^{+/+}$ mice (n = 8). (C) Fecal excretion of coprostanol (Copr), cholesterol (Chol) and

dihydroxy-cholesterol (DiH-Col) in L-*G6pc*$^{-/-}$ and L-*G6pc*$^{+/+}$ mice and C57BL/6 mice treated with either shChREBP or scrambled shRNA (n = 7-14). (D) Fecal energy excretion and (E) fecal fatty acid excretion in L-*G6pc*$^{-/-}$ and L-*G6pc*$^{+/+}$ mice and C57BL/6 mice treated with either shChREBP or scrambled shRNA (n = 7-14). Data represent Tukey boxplots. ***$p < 0.001$, *$p < 0.05$ indicates significance compared to wildtype littermates or scrambled shRNA.

Supplementary Tables

Table S1. Metabolic parameters in male C57BL/6 mice treated with S4048 or vehicle and in fasted L-*G6pc*$^{-/-}$ mice and wildtype littermates.

	C57BL/6 Vehicle Median (Range)	C57BL/6 S4048 Median (Range)	*p*-value	L-*G6pc*$^{+/+}$ Median (Range)	L-*G6pc*$^{-/-}$ Median (Range)	*p*-value
Body weight (g)	21.3 (20.1 – 23.4)	22.1 (18.7 – 24.9)	0.902	28.4 (21.5 – 29.9)	27.5 (25.3 – 32.5)	0.645
Liver weight (g)	1.0 (0.8 – 1.0)	1.3 (1.0 – 1.4	**0.009**	1.3 (0.8 – 1.5)	1.8 (1.6 – 2.0)	**<0.001**
Liver to body weight ratio (%)	4.3 (3.5 – 5.0)	5.6 (4.8 – 6.2)	**0.009**	4.4 (3.5 – 5.1)	6.7 (6.0 – 7.1)	**<0.001**
Blood glucose (mmol/L)	6.4 (4.1 – 6.9)	2.4 (1.7 – 2.9)	**0.001**	5.0 (3.7 – 8.4)	2.1 (1.7 – 2.4)	**<0.001**
Hepatic G6P (nmol/g liver)	67.1 (59.2 – 83.7)	128.9 (60.6 – 241.0)	0.051	421.7 (264.5 – 483.3)	2585.5 (1980.9 – 3457.3)	**<0.001**
Hepatic glycogen (mg/g liver)	2.2 (1.3 – 2.7)	39.8 (31.3 – 44.4)	**0.004**	17.7 (12.4 – 29.5)	54.2 (46.4 – 62.1)	**<0.001**
Glucagon (pg/mL)	138.4 (78.8 – 200.1)	225.4 (135.2 – 649.9)	**0.017**	112.7 (86.2 – 132.3)	235.9 (136.8 – 581.8)	**<0.001**
Insulin (ng/mL)	0.2 (0.1 – 0.3)	0.2 (0.1 – 0.3)	0.343	0.3 (0.1 – 0.6)	0.2 (0.1 – 0.4)	0.130

Table S2. Plasma and fecal bile acid profiles in L-*G6pc*$^{-/-}$ mice and wildtype littermates.

Bile acid species	L-*G6pc*$^{+/+}$ Median (Range)	L-*G6pc*$^{-/-}$ Median (Range)	*p*-value
Plasma (µmol/L)			
CA	0.41 (0.14 – 2.39)	0.46 (0.08 – 3.19)	1.000
TCA	0.26 (0.08 – 0.35)	0.65 (0.14 – 1.29)	0.281
DCA	0.62 (0.33 – 1.43)	0.30 (0.06 – 1.11)	0.232
TDCA	0.11 (0.06 – 0.18)	0.26 (0.09 – 0.34)	**0.021**
UDCA	0.14 (0.03 – 0.36)	0.09 (0.05 – 0.16)	0.497
TUDCA	0.04 (0.03 – 0.05)	0.05 (0.04 – 0.05)	1.000
CDCA	0.06 (0.02 – 0.14)	0.06 (0.02 – 0.10)	0.648
HDCA	0.07 (0.03 – 0.17)	0.05 (0.03 – 0.14)	0.921
THDCA	0.03 (0.03 – 0.03)	0.03 (0.03 – 0.03)	1.000
α-MCA	0.10 (0.05 – 0.19)	0.04 (0.03 – 0.09)	0.114
Tα-MCA	0.05 (0.01 – 0.07)	0.08 (0.01 – 0.12)	0.106
β-MCA	0.56 (0.14 – 2.63)	0.16 (0.03 – 0.89)	0.093
Tβ-MCA	0.10 (0.04 – 0.26)	0.06 (0.01 – 0.33)	0.649
ω-MCA	1.00 (0.48 – 4.25)	0.43 (0.11 – 1.75)	**0.040**
Total	3.14 (1.51 – 11.41)	2.62 (0.67 – 8.36)	0.232
Feces (µmol/day/100g BW)			
CA	0.57 (0.38 – 0.97)	1.01 (0.49 – 1.69)	**0.028**
UDCA	0.31 (0.19 – 0.51)	0.29 (0.20 – 0.36)	0.645
DCA	2.24 (1.61 – 3.99)	3.22 (1.92 – 4.54)	**0.050**
HDCA	0.23 (0.15 – 0.55)	0.20 (0.11 – 0.26)	0.161
α-MCA	0.66 (0.41 – 1.05)	0.74 (0.44 – 1.16)	0.574
β-MCA	0.96 (0.74 – 1.97)	0.61 (0.43 – 1.05)	**0.005**
ω-MCA	2.61 (1.84 – 4.03)	1.64 (0.78 – 2.00)	**0.001**
Total	7.71 (6.44 – 11.88)	8.14 (4.81 – 9.45)	0.878

Table S3. Biliary and plasma bile acid profiles in male C57BL/6 mice injected with either shChREBP or scramble AAV2/8 and treated with S4048 or vehicle.

Bile acid species	Scramble vehicle Median (Range)	Scramble S4048 Median (Range)	*p*-value	ShChREBP vehicle Median (Range)	ShChREBP S4048 Median (Range)	*p*-value
Bile (% of total)						
CA	0.56 (0.22 – 3.16)	2.95 (2.35 – 3.10)	0.073	0.75 (0.09 – 3.78)	1.38 (0.18 – 3.03)	0.833
GCA	0.13 (0.11 – 0.18)	0.18 (0.16 – 0.26)	0.109	0.08 (0.05 – 0.180	0.11 (0.09 – 0.12)	0.833
TCA	48.65 (46.70 – 62.57)	53.93 (43.28 – 56.99)	0.527	38.15 (24.71 – 47.28)	38.37 (32.47 – 45.77)	1.000
TDCA	2.17 (1.35 – 3.66)	3.80 (2.60 – 4.99)	**0.024**	0.58 (0.49 – 0.74)	0.83 (0.68 – 1.23)	0.067
TUDCA	1.00 (0.87 – 1.14)	1.00 (0.96 – 1.41)	0.648	1.09 (0.68 – 1.30)	1.09 (0.59 – 1.20)	0.833
TCDCA	0.98 (0.68 – 1.27)	1.10 (1.02 – 1.76)	0.315	1.57 (1.18 – 1.94)	1.79 (0.63 – 2.23)	0.833
THDCA	0.71 (0.28 – 1.58)	2.65 (0.77 – 3.25)	**0.024**	0.79 (0.16 – 1.69)	0.91 (0.19 – 1.15)	0.833
α-MCA	0.03 (0.00 – 0.38)	0.37 (0.21 – 0.38)	**0.024**	0.05 (0.00 – 0.39)	0.20 (0.00 – 0.64)	0.833
Tα-MCA	6.80 (5.32 – 8.16)	7.82 (6.96 – 8.55)	0.164	7.26 (5.65 – 9.15)	10.14 (4.61 – 10.88)	0.517
β-MCA	0.30 (0.08 – 0.85)	0.43 (0.25 – 0.75)	0.648	0.41 (0.14 – 1.58)	0.65 (0.18 – 0.99)	0.833
Tβ-MCA	35.84 (26.48 – 42.43)	23.65 (20.66 – 39.14)	0.073	45.12 (43.05 – 56.81)	46.89 (37.42 – 49.76)	1.000
ω-MCA	0.34 (0.23 – 1.09)	1.06 (0.59 – 1.72)	**0.042**	0.47 (0.22 – 1.81)	0.64 (0.18 – 2.75)	1.000
Plasma (µmol/L)						
CA	0.24 (0.14 – 0.71)	0.35 (0.11 – 10.10)	0.710	2.37 (0.21 – 44.60)	0.68 (0.25 – 4.65)	0.445
GCA	0.04 (0.04 – 0.16)	0.05 (0.03 – 0.09)	0.686	0.05 (0.03 – 0.24)	0.04 (0.04 – 0.05)	0.857
TCA	13.30 (0.17 – 65.20)	1.80 (0.14 – 37.00)	0.620	3.94 (0.94 – 31.70)	1.95 (0.47 – 17.30)	0.165
DCA	0.11 (0.07 – 0.57)	0.21 (0.10 – 3.08)	0.128	0.26 (0.06 – 0.99)	0.12 (0.05 – 0.46)	0.534
TDCA	0.24 (0.05 – 2.86)	0.14 (0.05 – 2.16)	0.805	0.14 (0.03 – 0.52)	0.12 (0.05 – 0.64)	1.000
UDCA	0.03 (0.03 – 0.05)	0.04 (0.03 – 0.26)	0.250	0.10 (0.05 – 0.52)	0.04 (0.03 – 0.07)	**0.015**
TUDCA	0.23 (0.03 – 0.87)	0.09 (0.03 – 0.48)	0.662	0.10 (0.04 – 0.63)	0.07 (0.04 - 0.33)	0.318
CDCA	0.05 (0.03 – 0.06)	0.09 (0.04 – 0.29)	0.400	0.12 (0.03 – 1.44)	0.06 (0.03 – 0.14)	0.394
TCDCA	0.20 (0.05 – 0.79)	0.17 (0.03 – 0.36)	0.730	0.08 (0.03 – 1.35)	0.05 (0.03 – 0.33)	0.383
HDCA	0.04 (0.03 – 0.06)	0.04 (0.04 – 0.16)	0.267	0.07 (0.03 – 0.32)	0.06 (0.03 – 0.16)	0.589
THDCA	0.07 (0.03 – 0.41)	0.10 (0.04 – 0.51)	0.445	0.14 (0.05 – 0.45)	0.06 (0.03 – 0.15)	0.101
α-MCA	0.04 (0.04 – 0.13)	0.14 (0.04 – 0.43)	0.229	0.22 (0.04 – 3.83)	0.05 (0.03 – 0.39)	0.836

Tα-MCA	1.36 (0.25 – 5.62)	0.28 (0.03 – 3.56)	0.295	0.83 (0.21 – 7.40)	0.17 (0.07 – 1.68)	0.073
β-MCA	0.22 (0.12 – 1.01)	0.26 (0.06 – 6.88)	0.805	1.53 (0.03 – 18.50)	0.69 (0.35 – 5.28)	0.165
Tβ-MCA	9.66 (0.07 – 52.60)	0.64 (0.11 – 39.80)	0.535	4.52 (1.56 – 59.00)	1.37 (0.31 – 26.50)	0.097
ω-MCA	0.51 (0.25 – 2.46)	0.89 (0.42 – 6.88)	0.318	1.42 (0.10 – 5.97)	1.03 (0.39 – 4.15)	0.535
Total	26.32 (1.27 – 133.43)	4.46 (1.30 – 98.50)	0.620	13.67 (3.80 – 166.63)	6.69 (3.18 – 51.00)	0.383

Table S4. Fecal bile acid profile in chow-fed C57BL/6 mice injected with either shChREBP or scramble AAV2/8.

Bile acid species	Scramble Median (Range)	shChREBP Median (Range)	*p*-value
Feces (µmol/day/100g BW)			
CA	1.48 (0.36 – 2.54)	1.03 (0.22 – 2.02)	0.210
DCA	1.55 (0.81 – 2.04)	0.92 (0.49 – 1.27)	**<0.001**
CDCA	0.07 (0.00 – 0.15)	0.00 (0.00 – 0.13)	0.743
α-MCA	0.40 (0.29 – 0.53)	0.31 (0.21 – 0.41)	**0.002**
β-MCA	0.83 (0.47 – 1.40)	0.93 (0.35 – 1.67)	0.210
ω-MCA	1.15 (0.66 – 1.58)	1.11 (0.52 – 1.78)	0.946
Total	5.31 (3.61 – 7.01)	4.61 (2.54 – 5.57)	0.085

Table S5. Biliary and plasma bile acid profiles in chow-fed L-*G6pc*$^{-/-}$ mice and wildtype littermates, injected with either shChREBP or scramble AAV2/8.

	L-*G6pc*$^{+/+}$ Scramble Median (Range)	L-*G6pc*$^{+/+}$ shChREBP Median (Range)	*p*-value	L-*G6pc*$^{-/-}$ Scramble Median (Range)	L-*G6pc*$^{-/-}$ shChREBP Median (Range)	*p*-value
Bile (% of total)						
CA	5.69 (1.97 – 7.32)	0.53 (0.00 – 3.46)	0.057	4.47 (3.64 – 7.80)	0.04 (0.00 – 0.22)	**0.016**
GCA	0.27 (0.11 – 0.30)	0.00 (0.00 – 0.11)	**0.029**	0.23 (0.21 – 0.39)	0.01 (0.00 – 0.09)	**0.016**
TCA	52.81 (46.69 – 59.94)	16.57 (10.70 – 29.58)	**0.029**	64.54 (50.90 – 68.52)	30.42 (25.20 – 41.08)	**0.016**
TUDCA	1.77 (1.01 – 2.35)	0.61 (0.21 – 1.19)	0.057	1.71 (0.46 – 2.10)	0.10 (0.00 – 0.22)	**0.016**
TCDCA	1.20 (0.48 – 1.79)	0.83 (0.45 – 1.11)	0.686	1.70 (0.38 – 1.94)	0.06 (0.00 – 0.13)	**0.016**
TDCA	1.83 (0.92 – 2.79)	0.06 (0.00 – 0.60)	**0.029**	1.22 (0.62 – 2.19)	0.01 (0.00 – 0.04)	**0.016**
THDCA	0.67 (0.45 – 1.16)	0.14 (0.00 – 0.39)	**0.029**	0.43 (0.24 – 0.68)	0.03 (0.00 - 0.07)	**0.016**
α-MCA	0.22 (0.06 – 0.53)	0.14 (0.00 – 0.34)	0.486	0.33 (0.14 – 0.72)	0.00 (0.00 – 0.01)	**0.016**
Tα-MCA	5.34 (3.30 – 8.70)	2.54 (0.76 – 4.80)	0.114	7.26 (2.71 – 7.98)	0.50 (0.42 – 0.68)	**0.016**
β-MCA	1.08 (0.31 – 1.74)	2.22 (0.00 – 4.40)	0.686	0.41 (0.32 – 1.07)	0.05 (0.00 – 0.49)	0.111
Tβ-MCA	26.41 (24.28 – 36.30)	75.66 (53.19 – 86.35)	**0.029**	19.37 (13.24 – 24.00)	68.67 (58.49 – 72.89)	**0.016**
ω-MCA	0.73 (0.25 - 2.19)	0.91 (0.00 – 1.93)	0.886	0.35 (0.23 – 0.77)	0.01 (0.00 – 0.13)	**0.016**
Plasma (µmol/L)						
CA	2.48 (1.51 – 3.44)	0.19 (0.19 – 0.19)	0.221	2.78 (2.03 – 3.28)	0.84 (0.82 – 24.00)	0.513
TCA	2.63 (0.73 – 4.54)	6.75 (6.74 – 6.76)	0.121	4.19 (1.63 – 5.14)	159.00 (39.20 – 250.00)	**0.050**
GCA	0.03 (0.02 – 0.03)	0.03 (0.02 – 0.04)	0.683	0.03 (0.02 – 0.04)	0.69 (0.27 – 1.42)	0.083
DCA	0.71 (0.42 – 1.00)	0.02 (0.01 – 0.03)	0.121	0.33 (0.29 – 0.52)	0.03 (0.02 – 0.03)	**0.050**
TDCA	0.14 (0.07 – 0.21)	0.03 (0.03 – 0.03)	0.121	0.11 (0.09 – 0.14)	0.11 (0.08 – 0.29)	1.000
UDCA	0.35 (0.27 – 0.43)	0.03 (0.03 – 0.03)	0.221	0.24 (0.17 – 0.33)	0.03 (0.03 – 0.03)	0.180
TUDCA	0.09 (0.05 – 0.14)	0.12 (0.11 – 0.14)	0.439	0.08 (0.06 – 0.10)	0.58 (0.35 – 0.82)	**0.050**
CDCA	0.13 (0.09 – 0.17)	0.04 (0.04 – 0.04)	0.221	0.13 (0.10 – 0.15)	0.01 (0.01 – 0.01)	**0.037**
TCDCA	0.05 (0.01 – 0.08)	0.21 (0.21 – 0.22)	0.121	0.07 (0.05 – 0.11)	0.53 (0.32 – 0.84)	**0.050**
GCDCA	0.01 (0.01 – 0.01)	0.01 (0.01 – 0.01)	0.121	0.01 (0.01 – 0.01)	0.02 (0.01 – 0.04)	**0.050**
HDCA	0.14 (0.10 – 0.17)	0.01 (0.01 – 0.01)	0.221	0.10 (0.08 – 0.11)	0.01 (0.01 – 0.03)	**0.046**

GHDCA	0.00 (0.00 – 0.00)	0.01 (0.01 – 0.010	0.121	0.00 (0.00 – 0.00)	0.10 (0.07 – 0.21)	**0.050**
THDCA	0.05 (0.03 – 0.06)	0.04 (0.04 – 0.04)	1.000	0.03 (0.02 – 0.07)	0.26 (0.17 – 0.35)	0.083
α-MCA	0.20 (0.07 – 0.32)	0.02 (0.02 – 0.02)	0.221	0.20 (0.17 – 0.21)	0.05 (0.02 – 0.08)	0.083
Tα-MCA	0.41 (0.14 – 0.68)	0.45 (0.35 – 0.55)	1.000	0.41 (0.14 – 0.42)	2.06 (1.41 – 4.28)	**0.050**
β-MCA	1.81 (1.27 – 2.35)	0.87 (0.15 – 1.60)	0.439	0.93 (0.93 – 1.62)	4.46 (1.43 – 18.70)	0.121
Tβ-MCA	1.24 (0.23 – 2.24)	36.80 (21.30 – 52.30)	0.121	0.93 (0.23 – 1.02)	322.00 (130.00 – 353.00)	**0.050**
ω-MCA	2.15 (1.46 – 2.84)	0.56 (0.09 – 1.04)	0.121	1.04 (0.87 – 1.16)	1.24 (0.38 – 8.58)	0.513
Tω-MCA	10.09 (3.78 – 16.40)	97.25 (70.50 – 124.00)	0.121	4.73 (2.48 – 5.77)	524.00 (168.00 – 1110.00)	**0.050**
Total	22.68 (10.26 – 35.09)	143.28 (102.51 – 187.05)	0.121	17.55 (10.11 – 18.20)	1012.28 (346.47 – 1772.22)	**0.050**

Table S6. Taqman and SYBR Green qPCR primer and probe sequences.

Gene	Species	Forward primer 5′-3′	Reverse primer 5′-3′	TaqMan probe 5′-3′
Primers for qPCR				
36b4	Mouse	GCT TCA TTG TGG GAG CAG ACA	CAT GGT GTT CTT GCC CAT CAG	TCC AAG CAG ATG CAG CAG ATC CGC
18S	Human	CGG CTA CCA CAT CCA AGG A	CCA ATT ACA GGG CCT CGA AA	CGC GCA AAT TAC CCA CTC CCG A
Cyp8b1	Mouse	AAG GCT GGC TTC CTG AGC TT	AAC AGC TCA TCG GCC TCA TC	CGG CTA CAC CAA GGA CAA GCA GCA AG
CYP8B1	Human	CCT GAG CTT GTT CGG CTA CAC	TGC GGA ACT CCA TGA ATA ACT CTC	CCT GTA GCA GGT CCT GCT CCT TGT CCT T
Cyp7a1	Mouse	CAG GGA GAT GCT CTG TGT TCA	AGG CAT ACA TCC CTT CCG TGA	TGC AAA ACC TCC AAT CTG TCA TGA GAC CTC C
CYP7A1	Human	TCA GCT TGG AAG GCA ATC CTA T	AGC CTC AGC GAT TCC TTG ATT A	CTG GCA GGT CAT TCA GTT CTG CTT GAC TC
Cyp7b1	Mouse	TGA AAT AGG AGC ACA TCA TCT TGG	AAT ACA TTG CCC AGA ACA TAG CTG	CTC TGG GCC TCT CTA GCA AAC ACC ATT C
CYP7B1	Human	CTT GAA ATA GGA GCA CAT CAT TTA GG	GAT AAT ACA TTG CCC AGA ACA TAG TTG	CTC TGG GCC TCT GTG GCA AAC ACT ATT C
Cyp27a1	Mouse	GCC TTG CAC AAG GAA GTG ACT	CGC AGG GTC TCC TTA ATC ACA	CCC TTC GGG AAG GTG CCC CAG
Cyp2c70[a]	Mouse	CCA CAG TGA AAT ATG GGC TTT T	AAT TTA GCT GTG ACT TCT GG	
ChREBPα	Mouse	CGA CAC TCA CCC ACC TCT TC	TTG TTC AGC CGG ATC TTG TC	CCT GGC TTA CAG TGG CAA GCT GGT CTC T
ChREBPα[a]	Human	AGT GCT TGA GCC TGG CCT AC	TTG TTC AGG CGG ATC TTG TC	
ChREBPβ	Mouse	TCT GCA GAT CGC GTG GAG	CTT GTC CCG GCA TAG CAA C	CTC AGT GGC AAG CTG GTC TCT CCC A
ChREBPβ[a]	Human	AGC GGA TTC CAG GTG AGG	TTG TTC AGG CGG ATC TTG TC	
Fxr	Mouse	CGC TGA GAT GCT GAT GTC TTG	CCA TCA CTG CAC ATC CCA GAT	ATG ATC ACA AGT TCA CCC CGC TCC TCT
Shp	Mouse	AAG GGC ACG ATC CTC TTC AA	CTG TTG CAG GTG TGC GAT GT	ATG TGC CAG GCC TCC GTG CC
Lrh-1	Mouse	TGC TGG AGT GAG CTC TTG ATT C	GAT GGT GGA GTA GTC CAC GTG T	CCT TCC TTC CCA TGC GCC ACT TG
Hnf4α	Mouse	ATG CCA AGG GGC TGA GTG AC	GCC GGT CGT TGA TGT AAT CCT	CAC CTG TGA CCG CAG CCG CTT G
L-PK	Human	TGT CTG TGC CAC ACA GAT GCT	CAT TGG CGA CAT CGC TTG TCT	CAT GAT TAC CAA GCC CCG GCC AAC
APOC3	Human	ATG AAG CAC GCC ACC AAG AC	TTG TCC TTA ACG GTG CTC CAG TA	CAC CCA GCC CCT GGC CTG CT
Mafg[a]	Mouse	CAA GGC CTT AAA GGT GAA GCG	TTC AAC TCT CGC ACC GAC AT	
Acly	Mouse	GGA GAA GTT GGG AAG ACC ACT G	CAA TGG CCG TCA TGT GAG TT	ATC CCC ATC CAT GTC TTT GGC ACA GA
Primers for subcloning				
ChREBPα		GCG AAA CTT AAG AGA TCT ATG GCG CGC GCG CT	GCG AAA GCG GCC GCG CTT GGA AAC TTT CAC CAG G	
ChREBPβ		GCG AAA CTT AAG ATG CGC GAA TAC CAC	GCG AAA GCG GCC GCG CTT GGA AAC TTT	

	AAG TGG A	CAC CAG G
Mlx	GCG AAA AAG CTT ATG GCC TAC CCA TAC GAC GT	GCG AAA CTC GAG TCA GTA GAG TTG GTT TTT CAA CTG

Table S7. SYBR Green primers used for ChIP-qPCR.

Region	Forward primer 5'-3'	Reverse primer 5'-3'
L-pk	GCT CTG CAG ACA GGC CAA AG	TCT TGC CAA TGG AAG CCT TG
Cyp8b1 region a[a]	GAG ACG AGG AAA GAG ATG TG	CAC CGA CTG CTC ACA TTC C
Cyp8b1 region b[a]	GAG CTG AAC CTG AAC AGT AG	CAG AGG CTC GGA CGT G
Cyp8b1 region c[a]	ACC ACG TCC GAG CCT CTG	GGA ATT GCT TTA TGT GGC
Cyp8b1 region d[a]	GGT GGG CTC AAG GCA G	GCT GAC TAG AGA GAC GAT G
Cyp8b1 region -2300	CTG CAG GAC AGA TTT CAT CTT G	TCA ACT GCA GAA TGT GTT AGG AC
Cyp8b1 region -1500	AGG CCC CAC AGA TAG ATT CA	CTG AGC ATC TGT CAG GGT GA
Cyp8b1 region -280	TAA GGA GAC ACC GTC TCT AC	GAG ACC TGA CAT CCC TCT AC
Cyp8b1 region -100	TTG CAG AGG ACG ATA CC	AAA GTG CGT GTC TGT G
Cyp8b1 region 1	CAG CGC TGT AGA GCT GAC AA	CAC TGT ACA CCA CAG CGT CA
Cyp8b1 region 500	TCC TGA GCT TAT TCG GCT ACA	CGG AAC TTC CTG AAC AGC TC
Cyp8b1 region 1000	CAG CGG ACA AGA GTA CCA GA	GGG GTC CAT GTG TAC TGA GAG
Cyp8b1 region 2000	CGA TGC CCT TAC TCC AAA TC	CTC GAT TCC ATT GAG CAA CA
Cyp8b1 region 5000	TGG AAG CTG CTG AGA AAG TG	CTC AGG TCC TGG CTT TTG TC

[a]Regions are explained in the manuscript